Arch. Metall. Mater. **64** (2019), 1, 119-123

DOI: 10.24425/amm.2019.126226

ZHIXIN TU*, JIANXIN ZHOU*#, YAJUN YIN*, XIAOYUAN JI*, XU SHEN*

THE DEVIATION FROM EUTECTIC COMPOSITION IN BOUNDARY LAYER FOR EUTECTIC GROWTH: A PHASE-FIELD STUDY

In this paper, the deviation from eutectic composition in boundary layer for eutectic growth is studied by phase-field method. According to a series of artificial phase diagram, the lamellar eutectic growth of these alloy is simulated during directional solidification. At steady state, average growth velocity of eutectic lamella is equal to the pulling velocity. With the increasing of the liquidus slope of β phase, the average composition in boundary layer would deviate from eutectic composition and the deviation increases. The constitutional undercooling difference between both solid phases caused by the deviation increases with the increasing of the deviation. The β phase would develop a depression under the influence of the deviation.

Keywords: Phase-field; Eutectic Growth; Solidification; Composition Deviation

1. Introduction

Eutectic is a significant microstructure in commercial alloys because the arrangement of a eutectic has a remarkable effect on their mechanical properties. The growth of lamellar eutectic, the most common eutectic, has been the subject for decades. Because the coupled eutectic growth is mainly influenced by diffusion and interface energy, the analytical solution of composition field is the key to describe the eutectic growth accurately. The steady-state solution for a lamellar and rod eutectic growth with a planar interface can be dated back to the time of Jackson and Hunt [1]. Based on this solution, they developed the theoretical analysis to the lamellar eutectic growth and achieved good accuracy. In the analysis, they argued that the average composition is approximately equal to the eutectic composition at solid-liquid interface regardless of the initial composition although it will slightly deviate from eutectic composition. However, the deviation is neglected in Jackson and Hunt analysis. But in their experiments [1], the continuous variation of composition in front of solid-liquid interface results in a series of eutectic with continuous lamellar spacing. It indicates the composition have a significant role on eutectic growth. Later, in the models for lamellar irregular eutectic [2-4], the steady-state solution of diffusion equation for planar interface is still used. The mainly difference between these models is the shape function for solid-liquid interface. The solution is still valid for most eutectic systems, and there are some difficulties in interpreting the irregular eutectic growth. Later, P. Magnin and R. Trivedi put forward a modification of the Jackson and Hunt theory [5,6], based on an equilibrium criterion for the triple-phase junction instead of the isothermal interface coupling condition. Although the steady-state solution of diffusion equation is also used, they argued that the deviation from eutectic composition in boundary layer should be responsible for the irregular growth in some eutectic alloys. As a result, the deviation cannot be neglected during eutectic growth analysis. In the latest studies by J.J. Xu et al. [7,8], the deviation reflects the interaction between the interface shape and the concentration field and effects the shape function of steady solid-liquid interface directly. Based on the above theoretical analyses, it is clear that the deviation from eutectic composition in boundary layer cannot be neglected.

In this paper, we used the phase-field method to study the composition field in boundary layer for lamellar eutectic growth during directional solidification [9-11], especially the deviation from eutectic composition in boundary layer and its influence on eutectic morphology. The deviation is validated by simulation and compared with existing theoretical predictions [5].

2. Simulation method

The multi-phase field model is chosen, which is originally established by Steinbach et.al and developed by Kim et.al and Eiken et al. [9-12]. The state of phase i with $\varphi_i = 1$ denotes the bulk phase. The sum of each phase field φ_i at any point is conserved throughout for a system with n phases:

$$\sum_i \varphi_i = 1 \tag{1}$$

* HUAZHONG UNIVERSITY OF SCIENCE AND TECHNOLOGY, STATE KEY LABORATORY OF MATERIALS PROCESSING AND DIE & MOULD TECHNOLOGY, WUHAN 430074, HUBEI PROVINCE, CHINA

Corresponding author: zhoujianxin@hust.edu.cn

In the case of a double obstacle potential, the free energy function of a system is given by

$$F = \int_V \left[\sum_{j>i} \sum_i \left(-\frac{\varepsilon_{ij}^2}{2} \nabla\varphi_i \nabla\varphi_j + \omega_{ij} \cdot \varphi_i \varphi_j \right) + \sum_i \varphi_i \cdot f^i(c_i) + \lambda_L \left(\sum_i \varphi_i - 1 \right) \right] dV \quad (2)$$

Where λ_L is a Lagrange multiplier which ensures the local sum of phase-field value equal to 1, ε_{ij}, ω_{ij} are gradient energy coefficient, height of double obstacle potential between two interacting phases i and j, $f^i(c_i)$ is the chemical potential for the bulk phase i.

A step function is defined, that is, $s_i = 1$ if $\varphi_i > 0$ and $s_i = 0$ otherwise. Then the number of nonzero phase-field variables coexisting at a given point is equal to the sum of s_i, that is, $n = \sum_i s_i$. The corresponding governing equation of phase field is given by

$$\frac{\partial\varphi_i}{\partial t} = -\frac{2}{n} \sum_{j\neq i}^{n} s_i s_j M_{ij} \left[\sum_{k\neq i}^{n} \left(\frac{\varepsilon_{ik}^2}{2} \nabla^2\varphi_k + \omega_{ik}\varphi_k \right) - \sum_{k\neq j}^{n} \left(\frac{\varepsilon_{jk}^2}{2} \nabla^2\varphi_k + \omega_{jk}\varphi_k \right) + \Delta G_{ij} \right] \quad (3)$$

where M_{ij}, ΔG_{ij} are phase-field mobility and driving force between phases i and j. M_{ij} can be calculated by

$$M_{ij} = 8\sigma_{ij} D \sqrt{2\omega_{ij}} \,/\, \left(\pi \Delta S_{ij} \cdot m_L \cdot \Delta c \cdot \varepsilon_{ij}^3 \right) \quad (4)$$

where

$$\varepsilon_{ij} = \frac{4}{\pi} \sqrt{\frac{\sigma_{ij}\eta}{2}} \quad (5)$$

$$\omega_{ij} = 4\sigma_{ij}/\eta \quad (6)$$

In the Eq. (4)-(6), σ_{ij}, η, ΔS_{ij}, D, m_L, Δc represent interfacial energy, interfacial width, transformation entropy, diffusion coefficient, slope of liquidus and composition difference between two phases, respectively. Here the solid state phase transformation is ignored. Therefore we simply assumed the phase-field mobility between two solid phases $M_{\alpha\beta} = (M_{\alpha L} + M_{\beta L})/2$ in present computation. The thermodynamic driving force ΔG_{ij} in Eq. (3) can be calculated by

$$\Delta G_{ij} = \left[T - T_E - m_L \left(c_L - c_L^E \right) \right] \cdot \Delta S_{ij} \quad (7)$$

where the term in square brackets of right hand is equal to the difference between liquidus and actual temperature T. And T_E, c_L, c_L^E are the eutectic temperature, phase composition for liquid, eutectic composition for liquid at $T = T_E$, respectively.

The diffusion equation is given as

$$\frac{\partial c}{\partial t} = \nabla \left(\sum_i \varphi_i D_i \nabla c_i \right) \quad (8)$$

where c_i is the phase composition, D_i is the diffusion coefficient in phase i. The coexisting phases at a point are assumed implicitly to have an equal diffusive potential. Average composition of the mixture also is given by a mixture rule

$$c = \sum_i \varphi_i c_i \quad (9)$$

where the phase composition c_i can be obtain combining with the assumptions of linear phase-diagram.

In the case of directional solidification, the initial temperature field follows the equation

$$T(x,z) = T_0 + G(z - z_0) \quad (10)$$

where z_0 is the reference position with temperature T_0, G is the temperature gradient in z-direction. The evolution equation is given as

$$\frac{\partial T}{\partial t} = -GV \quad (11)$$

which means that the temperature for the whole domain cools with a constant rate. V is the pulling velocity.

The phase diagram used in current simulation is shown in Fig. 1(a) and the parameters are list in Table 1. We chose the liquidus slope of β phase as variable, which varies from 80-800 K/mol. The sketch of initial condition is shown in

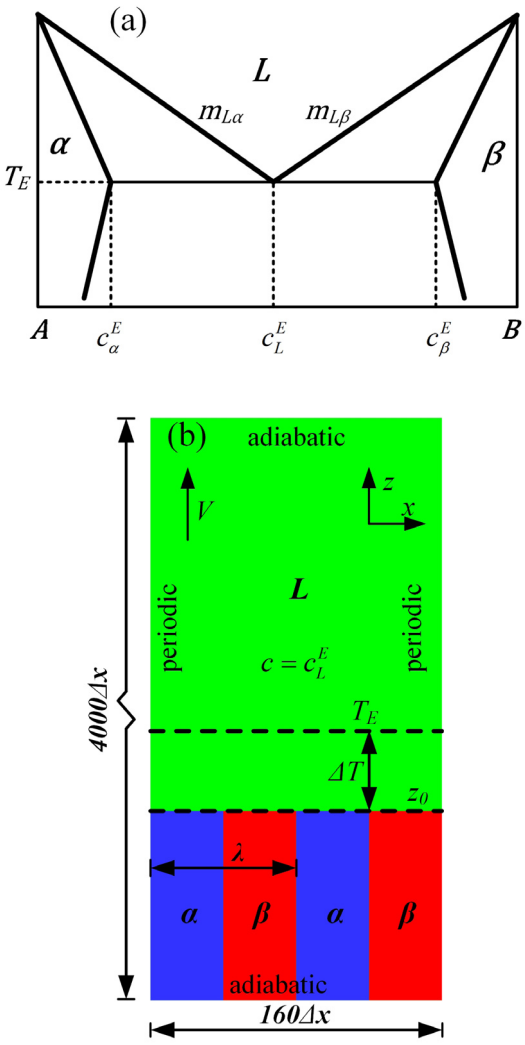

Fig. 1. Phase diagram used in simulation and the initial condition

Fig. 1(b). For all simulation cases, the initial liquid composition is set as eutectic composition. The initial lamellar spacing is set as lamellar spacing at minimum undercooling which is designated as $\lambda_{\min}$ and calculated by JH model [1]. In order to recover the Gibbs-Thomson effect with a good accuracy, $\lambda_{\min} = 80\Delta x$ and the interface width $\eta = 7\Delta x$. The domain size is fixed as $160\Delta x \times 4000\Delta x$, which contains two lamellar spacing. The pulling velocity V is 2 μm/s and the temperature gradient G is 10×10^3 K/m. For composition field and phase-field, a periodic boundary condition is imposed on the system boundaries parallel to the thermal gradient direction, while adiabatic condition on the other two boundaries.

TABLE 1

Physical properties used in the simulation

Symbol	Definition	Value
$\sigma_{\alpha L}$, $\sigma_{\beta L}$, $\sigma_{\alpha\beta}$	Interface energy	6×10^{-3} J/m^2
D_L	Liquid diffusivity	5×10^{-10} m^2/s
D_S	Solid diffusivity	5×10^{-14} m^2/s
$m_{L\alpha}$	Liquidus slope of α phase	80 K/mol
$m_{L\beta}$	Liquidus slope of β phase	80-800 K/mol
c_L^E	Eutectic composition of liquid	0.5
c_α^E	Eutectic composition of α phase	0.25
c_β^E	Eutectic composition of β phase	0.75
ΔS_α, ΔS_β	Entropy of fusion	2×10^4 J/(m^3·K)

3. Results and discussion

3.1. The establishing of steady state

Because the composition field and eutectic morphology at initial deviates from the steady state, there exists an adjustment before reaching steady state. Fig. 2 shows the adjustment of growth velocity and undercooling. During this transitional period, the practical growth velocity is lower than the pulling velocity. The liquid-solid interface recoils in the laboratory reference frame, which means that the undercooling increases. When reaching to steady state, average growth velocity is equal to the pulling velocity (2 μm/s) and average undercooling is equal to a constant. The phenomenon above consist with the real experimental results [13].

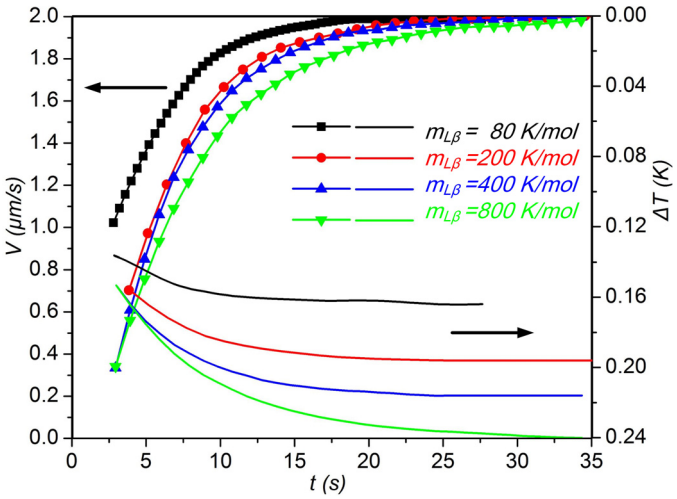

Fig. 2. Growth velocity and undercooling from initialization to steady-state

3.2. The composition field at steady state

The composition profiles along three horizontal lines, as designated by L_1, L_2, L_3 (see Fig. 3(a)) is shown in Fig. 3(b). The position of the line L_1 in Fig. 3(a) is through the tip of solid phase where $\varphi_L = 1$ is hold all the time. And if L_1 shifts a grid along negative z-axis, $\varphi_L = 1$ would not be hold at the tip of solid phase. As a result, the position of L_1 can prevent the influence of diffuse interface on results in phase-field method. Due to the periodicity of composition field along with x axis, composition profiles within a period are presented and they behaved in a form of the sinusoidal function approximately. And as the distance from the solid-liquid interface increases, the amplitude of composition profiles decreases. For each value of $m_{L\beta}$, the composition profiles intersect at a point. Because the volume fraction of α and β phase are equal to 0.5 in current simulation, the composition in the point is equal to the average composition in boundary layer. The average composition in boundary layer deviates from the eutectic composition as shown in Fig. 3(b). The difference between average composition and eutectic composition is designated by δC here. It is obvious that the value of δC increases with the increasing of $m_{L\beta}$.

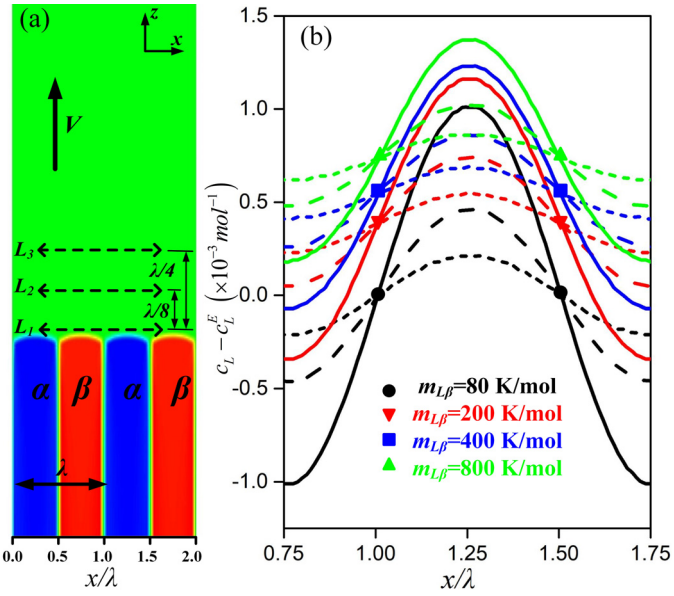

Fig. 3. Periodic composition field

In Fig. 4, it shows constitutional undercooling is discontinuous in the case of $m_{L\beta} = 200$ K/mol, where T_l^α and T_l^β are the liquidus temperature for α and β phase respectively. The constitutional undercooling ΔT_c and total undercooling ΔT is calculated

by the temperature and composition along L_1. ΔT_c is equal to $m_L(c_L - c_L^E)$ and ΔT is equal to the difference between eutectic temperature T_E and practical interface temperature T_i. According to the Gibbs-Thomson correction, total undercooling ΔT is equal to the sum of curvature undercooling ΔT_r and constitutional undercooling ΔT_c. So ΔT_r can be approximately estimated under the isothermal interface assumption. Constitutional undercooling is discontinuous because the composition in triple-phase junction is not equal to eutectic composition. The curvature undercooling is also discontinuous. The same phenomenon exists in the other cases when $m_{L\beta} \neq 80$ K/mol.

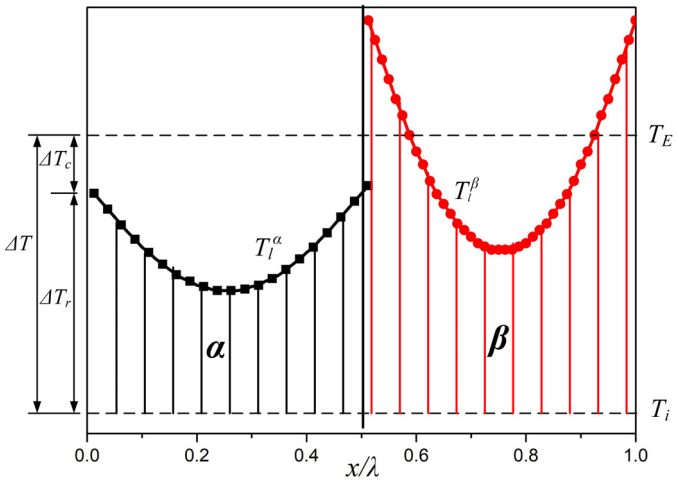

Fig. 4. The discontinuity of constitutional undercooling

In order to analyze δC, we give a quantitative comparison between the value of δC obtained by simulations and theoretical predictions. According to the model established by P. Magnin and R. Trivedi, δC can be expressed as [5]

$$\delta C = \left(\frac{f_\alpha}{m_{L\alpha}} - \frac{f_\beta}{m_{L\beta}} \right) \cdot \Delta T + \left(\frac{\sin\theta_\beta \cdot \Gamma_\beta}{m_{L\beta}} - \frac{\sin\theta_\alpha \cdot \Gamma_\alpha}{m_{L\alpha}} \right) \cdot \frac{2}{\lambda} \quad (12)$$

where f_α and f_β are the volume fraction, θ_α and θ_β are contacted angle, Γ_α and Γ_β are Gibbs-Thomas coefficient for α and β phase respectively, ΔT is the average undercooling. When calculating ΔT, the solid-liquid interface is defined as $\varphi_L = 0.5$ and ΔT is expressed as

$$\Delta T = \frac{1}{\lambda} \int_0^\lambda \left(T_E - T_i \left[z(x), x \right] \right) dx \quad (13)$$

where $T_i[z(x), x]$ is solid-liquid interface temperature, λ is the lamellar width, and $z(x)$ is the profile of solid-liquid interface. The simulated average undercooling ΔT is substituted into Eq. (12). As Fig. 5 shows, the undercooling and δC increase with $m_{L\beta}$ increasing. The value of δC by phase-field simulation agree with the value by theoretical prediction.

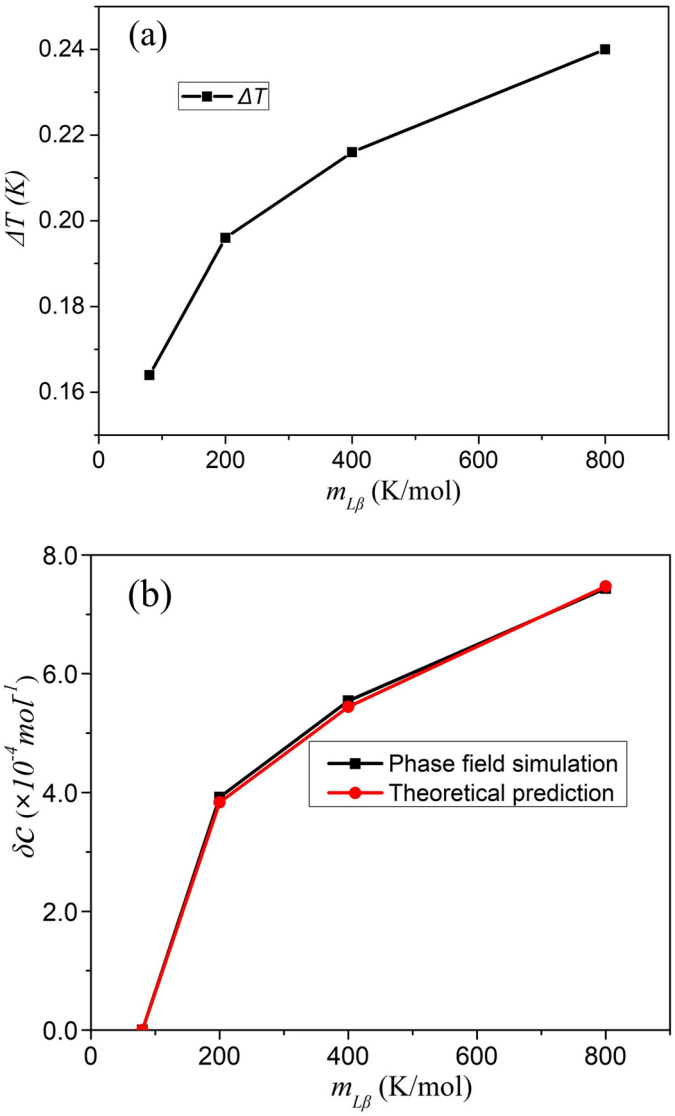

Fig. 5. The variation of undercooling and δC with the liquidus slope of β phase

3.3. The influences on lamellar morphology

Fig. 6 shows the lamellar morphology at steady-state with different value of $m_{L\beta}$. The outline is defined by $\varphi_i = 0.5$. As $m_{L\beta}$ increases, the lamellar morphology of α phase changes little. Nevertheless, it appears depression for β phase gradually. In Fig. 7, it shows the difference between the constitutional undercooling of both solid phases caused by δC which is quantified by $(|m_{L\alpha}| + |m_{L\beta}|)\delta C$. The constitutional undercooling difference increases with the increasing of δC. If the value of δC is equal to zero in the case of $m_{L\beta} > 80$ K/mol, the average constitutional undercooling of α phase will be raised, while that of β phase will be lowered. If the constitutional undercooling caused by δC is too high to be compensated by a curvature undercooling, the β phase would become more undercooled than α phase. It would result a non-isothermal solid-liquid interface. So the depression for β phase is more obvious with the increasing of $m_{L\beta}$.

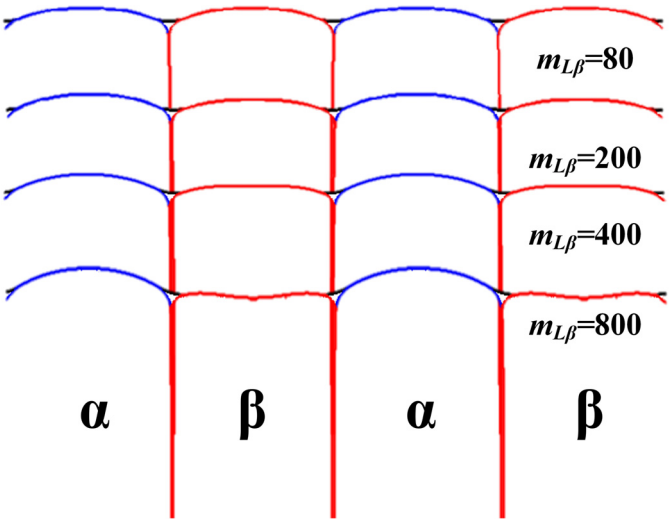

Fig. 6. Interface morphology at steady-state

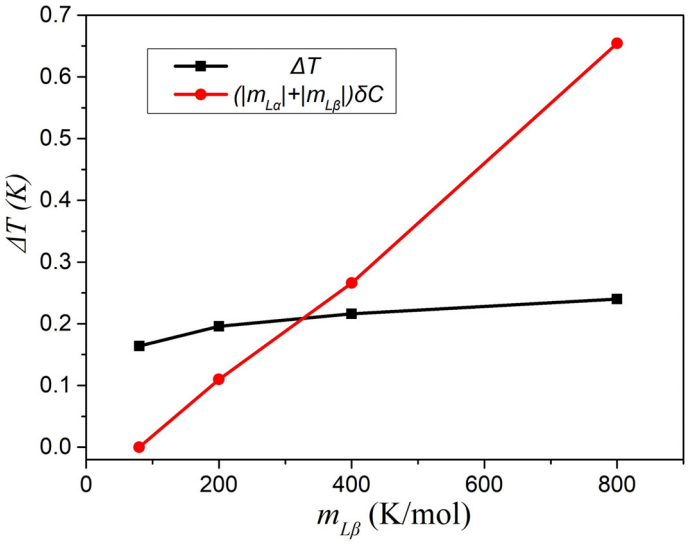

Fig. 7. Constitutional undercooling difference cause by deviation of boundary layer composition

4. Conclusion

1) At steady-state, average growth velocity is equal to the pulling velocity and average undercooling of solid-liquid interface is equal to a constant. The composition field would be stationary in the laboratory reference frame.
2) With the increasing of the liquidus slope of β phase, the average composition in boundary layer would deviate from eutectic composition and the deviation increase. The value of this deviation by phase-field simulation agrees with the theoretical prediction.
3) The constitutional undercooling difference between both solid phases caused by the deviation increase increases with the increasing of the deviation. The β phase would develop a depression under the influence of deviation if the constitutional undercooling difference could not be compensated by curvature undercooling.

Acknowledgements

This research is financially supported by a project aided by the National Nature Science Fund Projects of China (No. 51475181, No. 51605174).

REFERENCE

[1] K.A. Jackson, J.D. Hunt, Trans. Metall. Soc. AIME **236**, 1129-1142 (1966). DOI: 10.1016/B978-0-08-092523-3.50040-X
[2] D.J. Fisher, W. Kurz, Acta Metall. Mater. **28**, 777-794 (1980). DOI: 10.1016/0001-6160(80)90155-8
[3] P. Magnin, W. Kurz, Acta Metall. Mater. **35**, 1119-1128 (1987). DOI: 10.1016/0001-6160(87)90059-9
[4] E. Guzik, D. Kopyciński, Metall. Mater. Trans. A **37**, 3057-3067 (2006). DOI: 10.1007/s11661-006-0187-7
[5] P. Magnin, R. Trivedi, Acta Metall. Mater. **39**, 453-467(1991). DOI: 10.1016/0956-7151(91)90114-G
[6] P. Magnin, J.T. Mason, R Trivedi, Acta Metall. Mater. **39**, 469-480 (1991). DOI: 10.1016/0956-7151(91)90115-H
[7] J.J. Xu, Y.Q. Chen, Acta Mater. **80**, 220-238 (2014). DOI: 10.1016/j.actamat.2014.06.047
[8] J.J. Xu, X.M. Li, Y.Q. Chen, J. Cryst. Growth **401**, 93-98 (2014). DOI: 10.1016/j.jcrysgro.2013.11.050
[9] I. Steinbach, F. Pezzolla, B. Nestler, M. Seeßelberg, R. Prieler, G.J. Schmitz, J.L.L. Rezende, Phys. D, 94, 135-147 (1996). DOI: 10.1016/0167-2789(95)00298-7
[10] I. Steinbach, F. Pezzolla, Phys. D, **134**, 385-393 (1999). DOI: 10.1016/S0167-2789(99)00129-3
[11] S.G. Kim, W.T. Kim, T. Suzuki, M. Ode, J. Cryst. Growth **261**, 135-158 (2004). DOI: 10.1016/j.jcrysgro.2003.08.078
[12] J. Eiken, B. Böttger, I. Steinbach, Phys. Rev. E **73**, 66122 (2006). DOI: 10.1103/PhysRevE.73.066122
[13] M. Ginibre, S. Akamatsu, G. Faivre, Phys. Rev. E **56**, 780-796 (1997). DOI: 10.1103/PhysRevE.56.780